Sequence-dependent mechanics of single DNA molecules

Matthias Rief[1,2], Hauke Clausen-Schaumann[1] and Hermann E. Gaub[1]

[1]Lehrstuhl für Angewandte Physik, Amalienstraβe 54, 80799 München, Germany. [2]Present Address: Department of Biochemistry B400, Stanford University School of Medicine, Stanford, California 94305-5307, USA.

Atomic force microscope–based single-molecule force spectroscopy was employed to measure sequence-dependent mechanical properties of DNA by stretching individual DNA double strands attached between a gold surface and an AFM tip. We discovered that in λ-phage DNA the previously reported B-S transition, where 'S' represents an overstretched conformation, at 65 pN is followed by a nonequilibrium melting transition at 150 pN. During this transition the DNA is split into single strands that fully recombine upon relaxation. The sequence dependence was investigated in comparative studies with poly(dG-dC) and poly(dA-dT) DNA. Both the B-S and the melting transition occur at significantly lower forces in poly(dA-dT) compared to poly(dG-dC). We made use of the melting transition to prepare single poly(dG-dC) and poly(dA-dT) DNA strands that upon relaxation reannealed into hairpins as a result of their self-complementary sequence. The unzipping of these hairpins directly revealed the base pair–unbinding forces for G-C to be 20 ± 3 pN and for A-T to be 9 ± 3 pN.

With the development of piconewton instrumentation, mechanical experiments with individual molecules allow direct measurements of both inter- and intramolecular forces[1–5]. Conformational transitions in polymers[6,7] and unfolding of proteins[8–11] have been reported. Stretching experiments of λ-DNA[12–14] have revealed a highly cooperative transition at 65–70 pN, where B-DNA is converted into a new overstretched conformation called S-DNA. Theoretical descriptions and molecular-dynamics simulations have given insight into this process[15–17]. Unzipping experiments with single DNA molecules have been performed, and the correlation between the resulting force profile and the average G-C content in the strand demonstrated the potential of this kind of experiments for large-scale sequencing[18,19].

In this study we employed single-molecule force spectroscopy based on atomic force microscope (AFM) technology[20] to show that the mechanics of DNA overstretching is sequence dependent. Furthermore, we used this technique to measure directly the base-pairing forces of G-C and A-T nucleotides.

From a layer of DNA molecules adsorbed on a gold surface, an individual DNA strand was picked up with an AFM tip by applying a contact force of several nanonewtons (nN). Upon retraction, the DNA strand was stretched between gold surface and tip. The resulting force was measured through the deflection of the cantilever using optical lever detection. This attachment protocol has been shown to be applicable to a broad range of molecules and results in stable attachment under forces of up to a nanonewton[6–8].

In the extension/relaxation cycle of a 1.5 μm-long double stranded segment of digested λ-DNA (Fig. 1*a*), the well-known highly cooperative B-S transition can be observed at 65 pN. During this transition the helix elongates by nearly a factor of

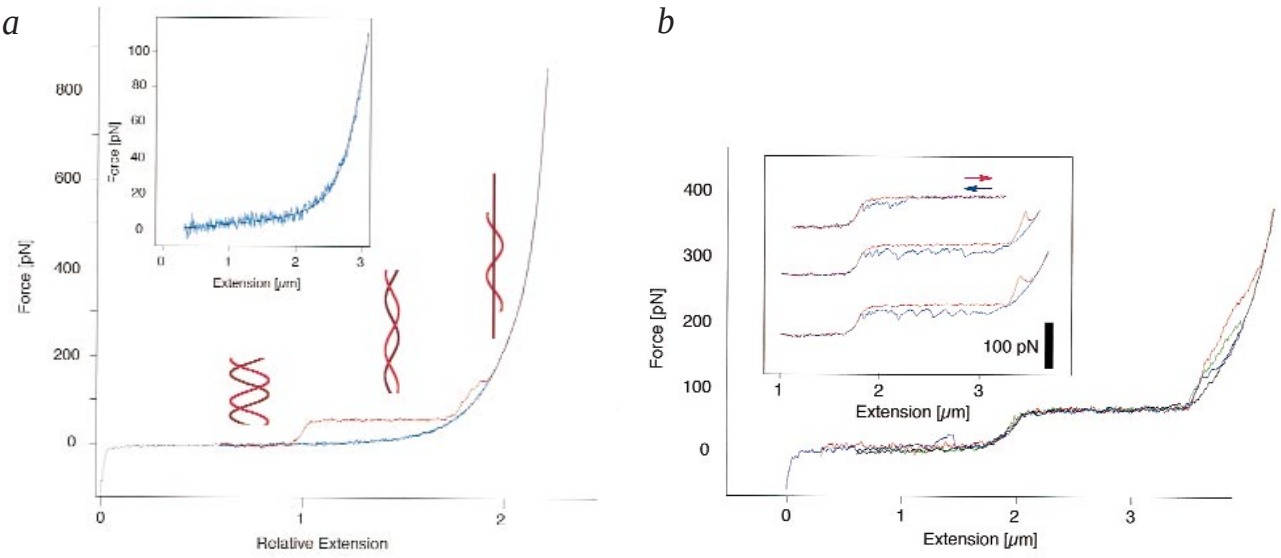

Fig. 1 Force-induced melting transition in λ-DNA. ***a***, Stretching (red) and relaxation (blue) curve of a 1.5-μm-long segment of a λ-BstE II digested DNA molecule. The superimposed black curve is a force curve taken on ssDNA. Because the ssDNA strand has a different contour length (~300 nm), the curves were scaled to the same contour length before superposition. Inset: low-force range of a relaxation curve of λ-DNA previously split in the melting transition (blue curve). The black curve is a fit according to the freely jointed chain model with an additional segment elasticity using the same parameters that have been determined for ssDNA[12] (Kuhn length 8 Å, molecular spring constant per unit length 800 pN). ***b***, Superposition of four extension traces of the same molecule taken at different pulling speeds (red, 3 μm s^{-1}; green, 1.5 μm s^{-1}; blue, 0.7 μm s^{-1}; black, 0.15 μm s^{-1}). Inset: a sequence of three stretching (red) and relaxation (blue) cycles performed each time on the same molecule (pulling speed: 0.25 μm s^{-1}). Partial melting of the double helix occurs during the B-S transition (first trace) and is complete after the melting transition (second and third trace). Reannealing of the two single strands leads to the characteristic shape of the relaxation traces.

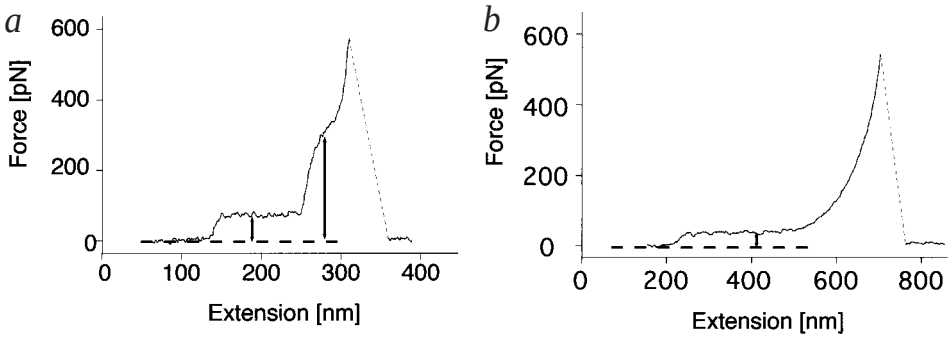

Fig. 2 The mechanical compliance of DNA strongly depends on the specific base pairing in the double helix. ***a***, For double-stranded poly(dG-dC) DNA the B-S transition occurs at 65 pN (see arrows), just as in λ-DNA, while the melting transition is raised to 300 pN, compared to 150 pN in λ -DNA. ***b***, In duplex poly(dA-dT) DNA the force of the B-S transition is reduced to 35 pN and the strands melt during this transition, so that no distinct melting transition can be observed (see Fig. 3).

two[12–14]. However, at forces of ~150 pN a new transition occurs, after which the force increases drastically upon further extension. Upon relaxation the force drops continuously and exhibits a marked hysteresis, indicating that a massive topological change occurs during this high force transition. A deformation trace of a ssDNA molecule that is free of hysteresis (black curve) was superimposed on the relaxation curve. The two curves are virtually indistinguishable. In fact, a fit of a polymer elasticity model to the low-force regime of the relaxation trace of a dsDNA molecule split in the high-force transition yields exactly the same parameters found for ssDNA by Smith *et al.*[12], who obtained ssDNA by denaturing dsDNA in distilled water or formaldehyde (Fig. 1*a*, inset). This agreement further corroborates our interpretation that the high-force transition is a force-induced melting transition in which the double helix is split into single strands.

Since the attachment forces for a single strand of DNA in our experiments hold up to more than a nanonewton, polymer elasticity models can now also be tested at high forces. The worm-like chain model and the freely jointed chain model, including an additional elastic modulus of 800 pN, yield equally good results in a force range up to 100 pN (Fig. 1*a*, inset). However, at higher forces these models fail to describe the measured force extension curves. It seems likely that quantum-mechanical *ab initio* calculations could provide new insights into the nonlinear enthalpic elasticity at high forces.The high attachment forces also show that the covalent bonds within a DNA strand are stable up to forces of at least a nanonewton, which is considerably higher than the 476 pN estimated by Bensimon *et al.*[14]

In some cases, (for example, the trace shown in Fig. 1*a*), permanent conversion to ssDNA occurs upon overstretching. It is possible that in this case a break in the DNA strand that melts off facilitates complete detachment of the strand and renders reannealing impossible. In many relaxation traces, however, reannealing into a complete double helix can be observed. In such a case (Fig. 1*b*), repeated splitting and reannealing can be performed several hundred times, using the same molecule. When four stretching curves recorded with the same molecule at different pulling speeds are superimposed (Fig. 1*b*), an interesting thermodynamic difference between the B-S transition and the melting transition can be observed: the force of the B-S transition proves to be independent of pulling speeds, whereas the melting transition exhibits a pronounced speed dependence. This shows that the B-S transition is an equilibrium process within the time scale of our experiment, whereas the melting transition occurs in nonequilibrium. In other words the rearrangement of the helix in the B-S transition occurs much faster than reannealing of the split strands.

A series of three extension/relaxation cycles, always performed on the same stretch of λ-DNA, is depicted in the inset of Fig. 1*b*. If the molecule is not stretched beyond the B-S coexistence plateau, the B-S transition is essentially reversible and shows only a small melting hysteresis (first trace). This small hysteresis may be due to partial melting of (presumably A-T-rich) regions in the DNA, as was already suggested by Smith and colleagues[12]. As soon as the molecule is stretched beyond the melting transition, the relaxation trace shows a pronounced reannealing hysteresis. The profile of the reannealing pattern is similar in traces recorded on the same DNA stretch (Fig. *1b*, inset, traces 2 and 3) but varies from stretch to stretch. This suggests that the reannealing profile is sequence dependent.

To obtain a more detailed understanding of the sequence dependence of the mechanical properties of DNA, we investigated synthetic constructs of double-stranded poly(dG-dC) as well as poly(dA-dT). We recorded extension traces where the molecules were stretched up to the maximum attachment force (Fig. 2). Upon detachment the lever snaps back to its resting position at zero force. The different sequences exhibit pronounced differences in their conformational transitions. For double-stranded poly(dG-dC) (Fig. 2*a*) the B-S transition occurs at 65 pN, just as in λ-DNA, while the melting transition is shifted toward higher forces starting at ~250 pN and leading into the single-stranded conformation at 350 pN. For poly(dA-dT) DNA (Fig. 2*b*), however, the B-S transition force is reduced to 35 pN and the double strand begins melting during this B-S transition, so that an additional melting transition can no longer be observed. This result can be explained by considering that the mechanical energy deposited in the double strand during the B-S transition (the area enclosed by the stretching and relaxation trace in Fig. 1*a*) already exceeds the base-pairing energy of poly(dA-dT).

When dsDNA of alternating G-C or A-T sequence is overstretched until the double helix melts, the resulting single strands can pair with themselves because of their self-complementarity. Consequently, the free strand, which is split off during the melting transition, should pair immediately into hairpins (see Fig. 3*a*). Thus reannealing of the two strands will be prevented upon relaxation of the strand that remains attached to the tip; instead, the attached strand will form a hairpin as well. Upon re-extension of the same molecule, the hairpin will be unzipped. This mechanism thus allows the measurement of the sequence-specific base-pairing forces in dsDNA.

The sequence of three extension/relaxation cycles of the same molecule of duplex poly(dG-dC) in Fig. 3*b* exhibits exactly this hairpin formation. In the first cycle the molecule is extended only into the B-S transition. Extension and relaxation traces exhibit a small amount of hysteresis. Despite this small hysteresis, no permanent conversion of the molecule has occurred dur-

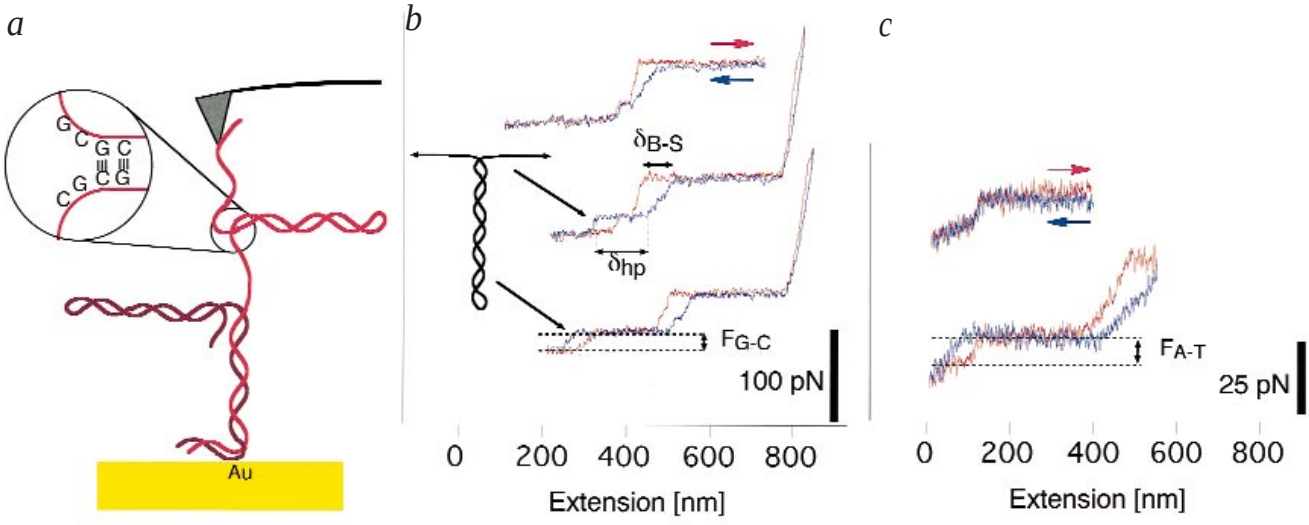

Fig. 3 Direct measurement of base-pairing forces. ***a***, The self-complementarity of poly(dG-dC) and poly(dA-dT) allows for hairpin formation within the two DNA strands. After force-induced melting of the double helix, base-pairing forces can be directly measured in the strand attached to the tip. ***b***, Three repeated extension (red) and relaxation (blue) curves of one poly(dG-dC) molecule. In the first extension/relaxation cycle, the molecule is extended into the B-S transition. This process is essentially reversible. In the second cycle the molecule is extended partly into the melting transition, which leads to a shortening of the B-S plateau and the appearance of a new plateau at $F_{G\text{-}C}$ = 20 pN in the relaxation trace, caused by hairpin formation. This 20 pN plateau reappears as a hairpin-unzipping plateau in the extension trace of the third cycle. Here the molecule is overstretched even more, resulting in further growth of the 20 pN plateau at the expense of the B-S plateau in the relaxation trace. ***c***, For poly(dA-dT) DNA the zipping/unzipping force is $F_{A\text{-}T}$ = 9 pN. The two plots show the stretching (red) and relaxation (blue) of a molecule that had already formed intrastrand hairpins during a previous stretching. The first cycle shows zipping and unzipping of the hairpins. In the second trace the double strand is further converted into intrastrand hairpins. The double helix starts to melt during the B-S transition.

ing this first cycle, as can be seen by noting that the extension trace of the second cycle is virtually identical to that of the first cycle. However, a small step at ~20 pN can be observed already in the first cycle, indicating a slight structural difference as compared to a fully double-stranded molecule (as in Fig. 2*a*). In the second force plot the molecule is partly extended into the melting transition. Here the relaxation trace shows a shortening of the B-S transition plateau and the appearance of a new plateau at a force of 20 pN. The length δ_{hp} (hairpin) of this new plateau is approximately twice as long as the length decrease $\delta_{B\text{-}S}$ in the B-S transition between the extension and relaxation curves. This is exactly what one expects if hairpins are formed. The 2:1 ratio is consistent with the contour length of ssDNA being approximately twice as long as the B-S plateau in dsDNA (see Fig. 1*a*). Therefore, we conclude that the new 20 pN plateau in the relaxation trace corresponds to the formation of hairpins that are unzipped in the subsequent extension trace.

The observation that hairpin formation occurs at a force that is well below the reannealing force of the double strand (Fig. 1*b*, inset) supports our assumption that hairpins are formed in the free strand as soon as it is melted off, thus blocking reannealing with the strand that is stretched. Consequently, upon relaxation less of the remaining DNA can recover to double-stranded conformation, so that it has to pair with itself and form hairpins as well. In the last plot (Fig. 3*b*), the same molecule is overstretched even further and again the 20 pN plateau grows at the expense of the B-S transition at a ratio of 2:1.

It can be seen in the second and third traces (Fig. 3*b*) that the 20 pN plateau appears at exactly the same force in both the stretching and relaxation cycles. Thus the zipping/unzipping transition occurs in thermodynamic equilibrium[18,19]. As a consequence, the zipping/unzipping forces do not depend on the pulling speed, as binding and unbinding of base pairs takes place on a much faster time scale than that of our experiment. It is to be expected, however, that in future experiments, using higher pulling speeds, a transition to a nonequilibrium regime will be observed, in which forces become speed dependent[22]. The lack of hysteresis in the plateau also shows that the hydrodynamic forces acting against the rotation of the B-hairpin during zipping and unzipping are much weaker than the base-pairing forces.

The same hairpin formation occurs in poly(dA-dT) DNA (Fig. 3*c*). The first extension/relaxation cycle shows the hairpin plateau of a DNA strand that already had partially melted during a previous extension. In the second trace additional duplex DNA is converted to ssDNA, forming hairpins upon relaxation. Here the zipping/unzipping plateau occurs at 9 pN. The hysteresis between extension and relaxation traces in this cycle shows that melting of the double strand in poly(dA-dT) occurs during the B-S transition.

From variations of unzipping force with average G-C content of λ-DNA, Essevaz-Roulet *et al.*[18] have extrapolated values for the unzipping forces of pure A-T and pure G-C base pairing of 10 pN and 15 pN, respectively. The differences between these estimates and unzipping forces of $F_{G\text{-}C} = 20 \pm 3$ pN and $F_{A\text{-}T} = 9 \pm 3$ pN presented here can be understood in the light of measurements of base-pairing free energies[23]. Free energy depends not only on the type of base pairing (A-T or G-C), but also on the sequence of bases itself. A poly(dA)poly(dT) duplex, for example, is much more stable than a poly(dA-dT) duplex like the one used in the experiments presented here. Knowing the unzipping forces of well-defined model sequences is thus an important step for large-scale sequencing of individual DNA molecules in mechanical experiments. Moreover, nano-mechanical experiments of the kind presented here can provide insight into a variety of biologically important structures like RNA secondary structure or RNA–DNA hybrids.

Methods

Sample preparation. λ-BstE II digested DNA (length distribution 117–8,454 bp) was purchased from Sigma (Deisenhofen, Germany). Duplex poly(dG-dC) (average length: 1,257 bp) and poly(dA-dT) (average length: 5,090 bp) were purchased from Pharmacia (Freiburg, Germany). In all preparation steps and experiments, Tris buffer containing 150 mM NaCl, 10 mM Tris (pH 8), 1 mM EDTA was used. DNA was allowed to adsorb onto a freshly evaporated gold surface from a 100 µl drop of a 100 µg ml^{-1} DNA solution (24 h incubation, ambient temperature). Alternatively, a 100 µl drop of a 100 µg ml^{-1} DNA solution was allowed to dry on the gold surface. Before beginning the experiment the sample was rinsed with buffer. Experiments were conducted at ambient temperature (20 °C).

Single-stranded DNA. Single-stranded DNA was obtained by dialyzing double-stranded λ-BstE II digested DNA against Millipore water. The sample was prepared as described. All preparation steps were carried out in Millipore water. Force measurements were conducted in Tris buffer (150 mM NaCl, 10 mM Tris, 1 mM EDTA, pH 8).

Force measurements. DNA molecules were picked up with an untreated Si_3N_4 AFM tip (Microlevers, Park Scientific Instruments). It has been shown in various studies that this nonspecific attachment holds forces of up to a nN[6–8]. Because the DNA molecules are not anchored at the ends, the apparent length of the molecule picked up varies. The extension of the molecule can be controlled with sub-angstrom precision with a piezo translator, and the force is measured by the deflection of the AFM cantilever spring. The spring constant of each lever was calibrated by measuring the amplitude of the thermal fluctuations[24,25]. Spring constants varied between 7 and 11 pN nm^{-1}; the resonance frequency of the cantilevers in buffer was between 700 Hz and 1 kHz. The measurements were carried out on a custom-built AFM. The sampling rate was 60 kHz. Each force curve consisted of 4,096 steps, and we recorded 10–200 data points per step depending on the desired pulling speed. A box-smoothing window (width: 20 steps) was applied to the data shown.

Correspondence should be addressed to H.E.G.
email: gaub@physik.uni-muenchen.de

Received 18 September, 1998; accepted 29 December, 1998.

1. Smith, S.B., Finzi, L. & Bustamante, C. *Science* **258**, 1122–1126 (1992).
2. Florin, E.-L., Moy, V.T. & Gaub, H.E. *Science* **264**, 415–417 (1994).
3. Lee, G.U., Chris, L.A. & Colton, R.J. *Science* **266**, 771–773 (1994).
4. Yin, H. *et al. Science* **270**, 1653–1657 (1995).
5. Kasas, S. *et al. Biochemistry* **36**, 461–468 (1997).
6. Rief, M., Oesterhelt, F., Heymann, B. & Gaub, H.E. *Science* **275**, 1295–1298 (1997).
7. Li, H., Rief, M., Oesterhelt, F. & Gaub, H.E. *Advanced Materials* **10**, 316–319 (1998).
8. Rief, M., Gautel, M., Oesterhelt, F., Fernandez, J.M. & Gaub, H.E. *Science* **276**, 1109–1112 (1997).
9. Tskhovrebova, L., Trinick, J., Sleep, J.A. & Simmons, R.M. *Nature* **387**, 308–312 (1997).
10. Kellermayer, M.S., Smith, S.B., Granzier, H.L. & Bustamante, C. *Science* **276**, 1112–1116 (1997).
11. Oberhauser, A.F., Marszalek, P.E., Erickson, H.P. & Fernandez, J.M. *Nature* **393**, 181–185 (1998).
12. Smith, S.B., Cui, Y. & Bustamante, C. *Science* **271**, 795–798 (1996).
13. Cluzel, P. *et al. Science* **271**, 792–794 (1996).
14. Bensimon, D., Simon, A.J., Croquette, V. & Bensimon, A. *Phys. Rev. Lett.* **74**, 4754–4757 (1995).
15. Lebrun, A. & Lavery, R. *Nucleic Acids Res.* **24**, 2260–2267 (1996).
16. Konrad, M.W. & Bolonick, J.I. *J. Am. Chem. Soc.* **118**, 10989–10994 (1996).
17. Ahsan, A., Rudnick, J. & Bruinsma, R. *Biophys. J.* **74**, 132–137 (1998).
18. Essevaz-Roulet, B., Bockelmann, U. & Heslot, F. *Proc. Natl. Acad. Sci. USA* **94**, 11935–11940 (1997).
19. Bockelmann, U., Essevaz-Roulet, B. & Heslot, F. *Phys. Rev. Lett.* **79**, 4489–4492 (1997).
20. Binnig, G., Quate, C.F. & Gerber, C. *Phys. Rev. Lett.* **56**, 930 (1986).
21. Xodo, L.E., Manzini, G., Quadrifoglio, F., van der Marel, G.A. & van Boom, J.H. *Biochemistry* **27**, 6321–6326 (1988).
22. Rief, M., Fernandez, J.M. & Gaub, H.E. *Phys. Rev. Lett.* **81**, 4764–4767 (1998).
23. Breslauer, K.J., Frank, R., Blöcker, H. & Marky, L.A. *Proc. Natl. Acad. Sci. USA* **83**, 3746–3750 (1986).
24. Florin, E.L. *et al. Biosens. Bioelectron.* **10**, 895–901 (1995).
25. Butt, H.-J. & Jaschke, M. *Nanotechnology* **6**, 1–7 (1995).